LA-UR- 98-3674

Approved for public release; distribution is unlimited.

Title: MODELING COMPACTION-INDUCED ENERGY DISSIPATION OF GRANULAR HMX

CONF-980803--

Author(s): K. A. GONTHIER
R. MENIKOFF
S. F. SON
B. W. ASAY

Submitted to: ELEVENTH INTERNATIONAL DETONATION SYMPOSIUM SNOMASS CONFERENCE CENTER, SNOWMASS, COLORADO
AUGUST 31 - SEPTEMBER 4, 1998

Los Alamos
NATIONAL LABORATORY

DISCLAIMER

DISCLAIMER

Portions of this document may be illegible in electronic image products. Images are produced from the best available original document.

MODELING COMPACTION-INDUCED ENERGY DISSIPATION OF GRANULAR HMX *

K. A. Gonthier †
Lamar University
Department of Mechanical Engineering
Beaumont, Texas 77710

R. Menikoff, S. F. Son and B. W. Asay
Los Alamos National Laboratory
Los Alamos, New Mexico 87545

A thermodynamically consistent model is developed for the compaction of granular solids. The model is an extension of the single phase limit of two-phase continuum models used to describe Deflagration-to-Detonation Transition (DDT) experiments. Our focus is on the energetics and dissipation of the compaction process. Changes in volume fraction are partitioned into reversible and irreversible components. Unlike conventional DDT models, the model is applicable from the quasi-static to dynamic compaction regimes for elastic, plastic, or brittle materials. When applied to the compaction of granular HMX (a brittle material), the model predicts results commensurate with experiments including stress relaxation, hysteresis, and energy dissipation. The model provides a suitable starting point for the development of thermal energy localization sub-scale models based on compaction-induced dissipation.

INTRODUCTION

Two-phase continuum models have been widely used to simulate Deflagration-to-Detonation Transition (DDT) in energetic granular solids [1, 2, 3]. Of this class of models, the Baer-Nunziato (BN) model [2, 4] is the most developed. It is based on mixture theory and is thermodynamically compatible. We adopt the framework of the BN model as a basis for analyzing compaction energetics in granular HMX. This work is motivated by the fact that compaction work is a dominant mechanism for hot-spot formation and thus plays a critical role in the weak initiation of DDT.

Changes in the internal energy of a granular solid due to compaction can be divided into two components: 1) an irreversible component which increases the thermal energy of the pure solid; and 2) a reversible component which is stored as recoverable energy. The recoverable energy enters the BN model as a potential in the Helmholtz free energy, and does not contribute to the thermal energy of the pure solid.

In the BN-model, the irreversible component is rate dependent and the reversible component is rate independent. In particular, all of the compaction energy for quasi-static compaction is predicted to be recoverable. This is at odds with quasi-static compaction experiments [5] for granular HMX which display a large hysteresis effect and imply that rate-independent compaction is mostly irreversible and thus thermal in nature. Moreover, the compaction potential of the BN model exceeds all plausible physical energy storage mechanisms; *e.g.*, recoverable shear strain energy. For dynamic compaction waves, the recoverable energy can be a significant fraction of the total compaction energy, though smaller than the dissipated energy.

In practice, contrary to the thermodynamic-based derivation of the BN model, computer code implementations of the model treat rate-independent compaction energy as thermal energy. The variation of the BN model formulated by Powers *et al.* (PSK) also thermalizes compaction energy.

In this work, we extend the thermodynamic formulation of the BN model to account for the hysteresis and stress relaxation observed in quasi-static compaction experiments. The main idea of this work

*This research is funded by the Department of Energy under Contract Number W-7405-ENG-36.

†Corresponding author: *gonthierka@hal.lamar.edu*

is to partition the volume fraction into elastic and inelastic components, and to then use this additional degree of freedom to obtain a better ansatz for the free energy. The extension is analogous to the formulation of models for elastic-plastic flow with work hardening. Our treatment of compaction is however much simpler than elastic-plastic flow because it is in the context of a hydrodynamic model in which the stress is a scalar rather than a tensor.

The following is an outline of the paper. First, we modify the free energy potential for the granular solid based on the partitioning of volume fraction, and propose an evolution equation for the inelastic component of volume fraction. Next, the dynamic compaction equations of the model are given and are shown to be consistent with the entropy inequality. Finally, the compaction energetics of granular HMX is described within the context of our model. This work is only the first step in developing an improved burn model that properly accounts for the energetics in a compaction wave. It also provides a thermodynamically consistent rationale for the computer implementation of the BN-model in practice, and for the PSK model.

FREE ENERGY

We focus on the solid phase of a granular material. In continuum hydrodynamic models, the thermodynamic state is characterized by a bulk (average) density ρ, bulk temperature T, and a solid volume fraction ϕ. For a densely packed granular solid, the initial porosity, $1-\phi$, is approximately 30%.

The BN-model is based on the principle of phase separation and in effect assumes the Helmholtz free energy is of the form [4]

$$\Psi(V,T,\phi) = \Psi_s(V_s,T) + B(\phi)\,, \tag{1}$$

where $V = 1/\rho$ is the specific volume of the granular solid, Ψ_s is the free energy of the pure solid, $V_s = 1/\rho_s = \phi V$ is the specific volume of the pure solid, and B is a potential for the compaction energy. The thermodynamic conjugate force to ϕ is called the configuration pressure β, and is defined by

$$\beta \equiv \rho\,\frac{\partial \Psi}{\partial \phi}\bigg|_{V_s,T} = \rho \frac{dB}{d\phi}\,. \tag{2}$$

Here, β can be interpreted as the average pressure resulting from the contact forces between grains, and thus models material strength within the context of a continuum fluid-like model. In order for the configuration pressure to be positive and monotonic, we require the compaction potential to be a convex function. In practice, β is measured in quasi-static compaction experiments and B is obtained by integrating β; *i.e.*, $B(\phi) = \int_{\phi_0}^{\phi} \frac{\beta}{\rho}\, d\phi$.

The form of the free energy determines the effective pressure of the material

$$P = -\,\frac{\partial \Psi}{\partial V}\bigg|_{T,\phi} = \phi P_s(V_s,T)\,. \tag{3}$$

The equilibrium volume fraction, determined by minimizing the free energy with respect to ϕ, corresponds to the condition for pressure equilibrium $P_s = \beta$. The compaction law used in the BN-model

$$\frac{d\phi}{dt} = g = \frac{\phi(1-\phi)}{\mu_c}(P_s - \beta) \tag{4}$$

amounts to a relaxation equation for pressure equilibrium because of the stiff dependence of the solid pressure P_s on its density $\rho_s = \rho/\phi$. The parameter μ_c has dimensions of dynamic viscosity (kg/m·s), and characterizes the relaxation time.

Thermodynamic consistency requires that the material specific energy is given by [4]

$$e = e_s(V_s,T) + B(\phi)\,, \tag{5}$$

where e_s is the specific energy of the pure solid. Consequently, within the formulation of the BN-model, the energy associated with changes in volume fraction due to quasi-static compaction is reversible. However, quasi-static compaction experiments [5] display a large hysteresis effect. In particular, when a sample of granular material is compacted to low porosity and then unloaded, ϕ does not return to its initial value. This is indicative of substantial irreversibility. Moreover, the experimental value of the quasi-static compaction energy needed to completely squeeze out the pores (*i.e.*, $\int_{\phi_0}^{1} \frac{\beta}{\rho}\, d\phi$) is for HMX on the order of 5 J/g. The maximum energy associated with shear strain is determined by the yield strength and the shear modulus and is less than 1 J/g. Since the quasi-static compaction energy exceeds the amount of energy that can be stored as a potential, most of the compaction energy must be dissipated as heat. Both sliding friction between grains and plastic work are likely dissipative mechanisms in the compaction process.

Code implementations of the BN-model use for the pressure $P = \phi P_s(V_s,e)$. This corresponds to the material specific energy being $e = e_s$ without the compaction potential in Eq. (5). In the regime where compaction is of interest, the pure solid equation of state is very stiff and thus the pressure is dominated by small changes in the density. Consequently, the

compaction energetics has only a small effect on the mechanical behavior of a compaction wave [4]. Furthermore, the bulk temperature rise in a compaction wave is small and reaction rates are empirically fit to depend mainly on the pressure which is insensitive to the treatment of compaction energy. The energetics of a compaction wave will however be important for developing improved burn models.

In order to reconcile the quasi-static compaction experiments with the model, the free energy must be modified. Compaction experiments show that loading leads to a change in grain morphology; grains can fracture, distort plastically and rearrange their positions leading to a lower stress-free porosity. This motivates introducing an additional variable $\tilde{\phi}$ to characterize the no-load volume fraction. In analogy with elastic-plastic theory [6], we shall interpret $\tilde{\phi}$ as representing the inelastic, or irreversible, component of the volume fraction and $\phi - \tilde{\phi}$ as representing the elastic, or reversible, component of the volume fraction.

As an ansatz we assume that the compaction potential depends only on the elastic component of the volume fraction. This leads to a modified free energy of the form

$$\Psi(V, T, \phi, \tilde{\phi}) = \Psi_s(V_s, T) + B(\phi - \tilde{\phi}) \,. \qquad (6)$$

We define the conjugate thermodynamic force to $\tilde{\phi}$ to be

$$\tilde{\beta} \equiv -\rho \left. \frac{\partial \Psi}{\partial \tilde{\phi}} \right|_{V_s, T, \phi} \,. \qquad (7)$$

Here, $\tilde{\beta}$ is the analog of a "plastic" stress. Since B depends only on the elastic volume fraction, it follows from Eq. (2) that $\tilde{\beta} = \beta$. In addition, the specific energy of the material depends on the elastic volume fraction rather than the total volume fraction, *i.e.,*

$$e = e_s(V_s, T) + B(\phi - \tilde{\phi}) \,. \qquad (8)$$

Later we will check that our modification to the model satisfies the entropy inequality. Here we note that the differential form of the fundamental thermodynamic relation is given by

$$T d\eta = P dV + de + (P_s - \beta) V d\phi + \beta V d\tilde{\phi} \,, \qquad (9)$$

where $\eta = -(\partial/\partial T)\Psi$ is the entropy. It is important to note that $\eta = \eta_s(V_s, T)$; thus, the material specific entropy is identical to the entropy of the pure solid. Terms in the thermodynamic relation proportional to β are a consequence of the potential energy term in Eq. (8).

Having introduced a new thermodynamic state variable, we need to specify an evolution equation for $\tilde{\phi}$. We assume that

$$\frac{d\tilde{\phi}}{dt} = \tilde{g} = \begin{cases} \dfrac{1}{\tilde{\mu}(g)}[f(\phi) - \tilde{\phi}] & \text{if } f(\phi) > \tilde{\phi}, \\ 0 & \text{otherwise.} \end{cases} \qquad (10)$$

This form for $\tilde{g}$ can be interpreted analogously to the dynamics of plastic strain for rate-dependent elastic-plastic flow. The function $f(\phi)$ represents the yield surface for the inelastic volume fraction and the dependence of the yield surface on ϕ represents work hardening. The parameter $\tilde{\mu}$ characterizes the relaxation time for $\tilde{\phi}$ to return to the yield surface.

In the elastic regime, $\tilde{\phi} \le \phi < f^{-1}(\tilde{\phi})$, $d\tilde{\phi}/dt = 0$ and the pressure equilibrium condition is as before, $P_s = \beta = \rho B'(\phi - \tilde{\phi})$, except that the configuration pressure now depends on both ϕ and $\tilde{\phi}$. The dynamics constrain $\tilde{\phi}$ to be non-decreasing in the inelastic regime. Consequently, from Eq. (9) the entropy can only increase as $\tilde{\phi}$ evolves. Moreover, we see from Eq. (8) that increasing $\tilde{\phi}$ has the effect of transferring compaction potential energy to thermal energy. The energetics implemented in codes, namely $e = e_s$, correspond to $f(\phi) = \phi$ in the limit that $\tilde{\mu} \to 0$. The limit of zero relaxation time for the return to the yield surface is analogous to rate-independent plasticity.

MATHEMATICAL MODEL

The equations for the flow of a granular material are an extension of the fluid equations. These consist of conservation of mass, momentum and energy

$$\frac{\partial}{\partial t}\begin{pmatrix} \rho \\ \rho u \\ \rho E \end{pmatrix} + \frac{\partial}{\partial x}\begin{pmatrix} \rho u \\ \rho u^2 + P \\ \rho u(E + PV) \end{pmatrix} = \vec{0} \,, \qquad (11)$$

where the total specific energy is $E = e + \frac{1}{2}u^2$, plus rate equations for the total volume fraction

$$\frac{d}{dt}\phi = g \qquad (12)$$

and the inelastic component of the volume fraction

$$\frac{d}{dt}\tilde{\phi} = \tilde{g} \,, \qquad (13)$$

together with the constitutive relation defining the pressure $P = \phi P_s(V_s, e_s)$ where $V_s = \phi/\rho$ and $e_s = e - B(\phi - \tilde{\phi})$. The fluid equations and the rate equations are coupled through the source terms and the algebraic constitutive relations. Apart from the addition of $\tilde{\phi}$ these equations correspond to the single phase limit of both the BN [4] and PSK [7] models.

Additionally, we need to specify the rate functions for the compaction dynamics. As in the BN-model, we assume that the dynamics of the total volume fraction is governed by g as in Eq. (4), but with a slight modification:

$$g = \begin{cases} \dfrac{\phi(1-\phi)}{\mu_c}\Big(P_s - \beta\Big) & \text{if } \phi > \tilde{\phi}, \\ 0 & \text{otherwise,} \end{cases} \tag{14}$$

where $\beta = \rho B'(\phi - \tilde{\phi})$. This modification restricts ϕ to be greater than $\tilde{\phi}$ as is required by our underlying micro-mechanical view of the material. For the inelastic component of the volume fraction, we assume that $\tilde{g}$ is given as in Eq. (10), and that the relaxation parameter is given by

$$\frac{1}{\tilde{\mu}(g)} = \frac{1}{\tilde{\mu}_0}\left(1 + \frac{\tilde{c}|g|}{\tilde{\mu}_0}\right), \tag{15}$$

where the constants $\tilde{\mu}_0$ and $\tilde{c}$ are material-dependent parameters that characterize the slow and fast response, respectively.

In the previous section, we discussed the energy and dissipation associated with the compaction potential $B(\phi)$ in the free energy. The dynamics of the model contains an additional rate-dependent dissipative term that is important for compaction waves. Combining the fundamental thermodynamic relation, Eq. (9), with the dynamical equations for the model, Eqs. (11)–(13), we find that the dissipation is given by

$$\begin{aligned} T\frac{d\eta}{dt} &= P_s\frac{dV_s}{dt} + \frac{de_s}{dt} \\ &= \underbrace{(P_s - \beta)V\frac{d\phi}{dt}}_{\text{(i)}} + \underbrace{\beta V\frac{d\tilde{\phi}}{dt}}_{\text{(ii)}}. \end{aligned} \tag{16}$$

The first term (i) is present in the standard BN-model. This term is non-negative because the compaction rate g is chosen such that $P_s - \beta$ and $d\phi/dt$ have the same sign. For a quasi-static compaction process, both $d\phi/dt \to 0$ and $P_s - \beta \to 0$. Consequently, this term has a negligible affect on slow flow, though it can provide substantial dissipation for fast flow such as occurs in the rapid rise of a compaction wave profile.

The second term (ii) results from our modification to the model. This term is non-zero since both $\beta \geq 0$ and $d\tilde{\phi}/dt \geq 0$. For a slow process βV can be non-zero and this term will raise the entropy proportional to the change in $\tilde{\phi}$. Thus, it will cause quasi-static compaction to be dissipative and irreversible. Since it converts recoverable energy to thermal energy, the second term also contributes to the dissipation in a compaction wave. For fast processes, β is not in equilibrium with respect to $\tilde{\phi}$ and thus the second term also can be compaction rate-dependent. However, the distinguishing property of the second term is that its time integral does not vanish for quasi-static compaction.

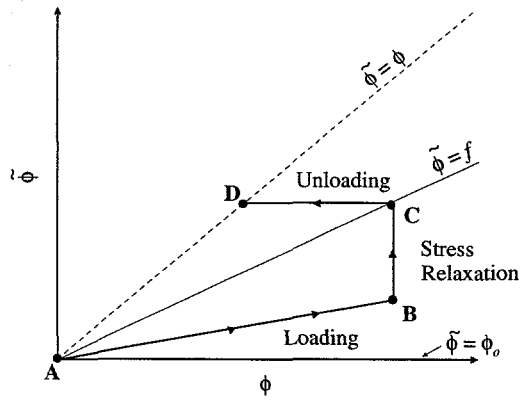

FIGURE 1. A HYPOTHETICAL LOADING, STRESS RELAXATION, AND UNLOADING COMPACTION PROCESS.

The modified model is compatible with the hysteresis and stress relaxation observed in quasi-static compaction experiments [5]. Shown in Fig. 1 is a simple schematic of a hypothetical loading, stress relaxation, and unloading quasi-static compaction process in the $(\phi, \tilde{\phi})$-plane. For purposes of illustration, we have chosen the equilibrium no-load volume fraction, $f(\phi)$, to be a linear function passing through point **A**, the initial loosely packed unstressed state with $\tilde{\phi} = \phi = \phi_0$.

During the loading process from point **A** to point **B**, ϕ increases faster than $\tilde{\phi}$ leading to an increase in β. At point **B**, the loading is stopped and sufficient force is applied to maintain a constant volume; the volume fraction ϕ is nearly constant because the solid has a stiff equation of state. However, **B** is outside the elastic region, bounded by the lines $\tilde{\phi} = \phi$ and $\tilde{\phi} = f$, and is not an equilibrium state. Consequently, $\tilde{\phi}$ continues to increase as the material relaxes to the boundary of the elastic region, $\tilde{\phi} = f$, at point **C**. This is a period of stress relaxation since $\phi - \tilde{\phi}$, and hence β, decreases. During stress relaxation some of the stored recoverable energy is thermalized, *i.e.*, $\Delta e_s = B(\phi_B - \tilde{\phi}_B) - B(\phi_C - \tilde{\phi}_C)$. The increase in $\tilde{\phi}$ is irreversible.

Subsequently, suppose the force maintaining the volume fraction is removed. During the

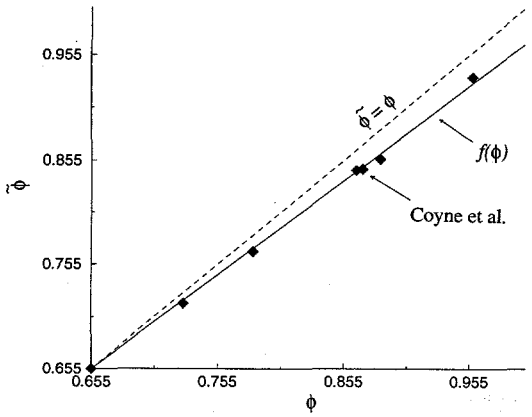

FIGURE 2. VARIATION OF $\tilde{\phi}$ WITH ϕ BASED ON QUASI-STATIC COMPACTION EXPERIMENTS.

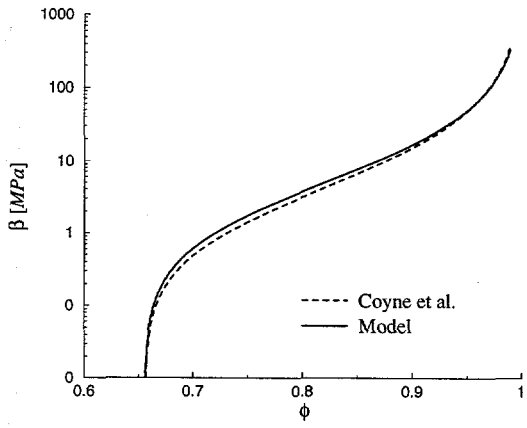

FIGURE 3. VARIATION OF β WITH ϕ BASED ON QUASI-STATIC COMPACTION EXPERIMENTS.

unloading process from point **C** to point **D**, ϕ decreases until it equals $\tilde{\phi}$. The remaining stored recoverable energy $B(\phi_C - \tilde{\phi}_C)$ is released. This reversible component of the compaction energy is only a fraction of the energy supplied during the loading stage. Moreover, at the stress-free end state, point **D**, $\tilde{\phi}$ is larger than its value at the start of the loading process. Hysteresis is the failure of ϕ to return to its initial value, and is a consequence of the dissipation resulting from the change of the internal variable $\tilde{\phi}$.

In summary, our extension of the BN-model describes both an elastic compaction region, $\tilde{\phi} \leq \phi \leq f^{-1}(\tilde{\phi})$, and an inelastic compaction region, $\phi > f^{-1}(\tilde{\phi})$. This is quite analogous to elastic-plastic flow. The inelastic region is responsible for the hysteresis effect observed in quasi-static compaction experiments.

COMPACTION OF GRANULAR HMX

In this section, we apply the model to both quasi-static and dynamic compaction of granular HMX. It is not the intent of this section to give a detailed analysis of granular HMX compaction; rather, we simply give an application of the model, noting salient features, and determine constitutive relations appropriate for granular HMX to be used in future work.

As is routinely done in the absence of dynamic compaction data, we determine constitutive relations based on quasi-static compaction experiments, and apply these relations to dynamic compaction. To this end, we use the quasi-static compaction data reported by Coyne *et al.* [5] for coarse HMX. In their experiments, Coyne *et al.* quasi-statically loaded and unloaded small samples of granular HMX contained within a movable piston-fixed cylinder apparatus. Each loaded sample was allowed to undergo stress relaxation prior to unloading. Granular bed displacement, applied stress, and transmitted stress were simultaneously recorded. Based on 1) the rebound of the granular bed upon unloading and 2) the maximum volume fraction prior to unloading, the equilibrium no-load volume fraction, $f(\phi)$, can be estimated. The results, summarized in Fig. 2, indicate that f can be taken as a linear function of ϕ through the ambient state. The resulting expression for f is

$$f(\phi) = \phi_0 + c(\phi - \phi_0), \tag{17}$$

where $c = 0.913$ and $\phi_0 = 0.655$. Also, based on the stress measurements of Coyne *et al.*, we approximate the configuration pressure by

$$\beta(\phi, \tilde{\phi}) = \beta_0 \, \phi \, h(\phi - \tilde{\phi}) \tag{18}$$

where $\beta_0 = 1.49\,\text{MPa}$,

$$h(\phi_e) = -\phi_e \frac{\ln(\kappa - \phi_e)}{\kappa - \phi_e}, \tag{19}$$

and $\kappa = 0.03$. The density dependence of β is ignored because, for the regime in which compaction is important, the pressure is low compared to the bulk modulus and thus the density is nearly constant. A comparison between the experimental stress data and the fit given by Eq. (18) is shown in Fig. 3.

We now estimate values for the parameters $\tilde{\mu}_0$ and $\tilde{c}$ in Eq. (15) based on the simulation of quasi-static compaction experiment HMX-23 reported by Coyne *et al.* The simulation consists of a (**I**) loading, (**II**) unloading, and(**III**) reloading cycle at a constant

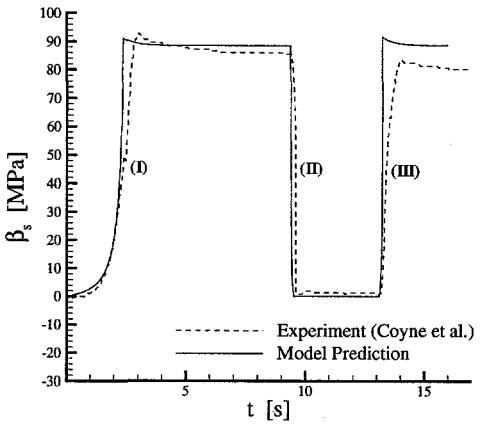

FIGURE 4. PREDICTED AND EXPERIMENTAL STRESS HISTORY FOR THE QUASI-STATIC COMPACTION OF GRANULAR HMX.

extension rate of 18.8 cm/s during loading and reloading. We take $\tilde{\mu}_0 = 0.5\,\mathrm{s}$ and $\tilde{c} = 1.461 \times 10^4\,\mathrm{s}^2$. A comparison of the computed and experimental results is shown in Fig. 4. Here, $\tilde{c}$ is determined based on the loading portion of the cycle, whereas $\tilde{\mu}_0$ is chosen based on the time scale of the stress relaxation process immediately following cessation of loading. It is noted that only the extrema of t and β were reported for the stress history shown in Fig. 1 of reference [5]. We linearly scaled these values between their extrema to obtain the experimental history shown in fig. 4; as such, these results should be interpreted as semi-quantitative. Neither the BN model [2], which predicts full material recovery, nor the PSK model [3], which predicts no material recovery, correctly models the compaction behavior of granular HMX in this slow compaction limit. Additionally, neither model predicts the observed stress relaxation.

With all model parameters fixed, we now apply the model to the dynamics of a steady compaction wave. For brevity, details of this analysis are not given as comparable analyses are published elsewhere in the literature [8, 7]. The analysis assumes a steady wave propagating to the right with speed D, and re-expresses the governing equations in a reference frame propagating with the wave. We make two additional simplifications. First, we assume that the solid grains are incompressible, and restrict the analysis to compaction waves propagating with speeds much less than the ambient solid acoustic speed ($D < 800\,\mathrm{m/s} < \mathrm{c} \approx 2600\,\mathrm{m/s}$). Second, since the non-dimensional quantity $\tilde{c}/\tilde{\mu}_0^2$ is large (5.844×10^4), we replace Eq. (10) with the equilibrium condition $\tilde{\phi} = f(\phi)$. Thus, the steady problem can be reduced to a single ordinary differential equation for ϕ, with all remaining system variables expressed in terms of ϕ.

Figure 5 summarizes predictions of the dynamic compaction wave analysis for $\phi_0 = 0.73$. Shown in Fig. 5(a) and 5(b) are the predicted variation with piston velocity of the compaction wave speed and volume fraction behind the wave. Also shown in these figures are dynamic compaction data for granular HMX obtained by Sandusky *et al.* [9], as reported by Baer [8]. Reasonable agreement exists between the computed and experimental results.

More interesting is Fig. 5(c) showing the predicted variation with piston velocity of 1) the specific compaction work w_c, obtained by integrating the specific internal energy e through the wave profile, and 2) the fraction of w_c corresponding to the dissipative terms **(i)** and **(ii)** in Eq. (16), and the recoverable compaction energy. As evident in the figure, very little of the total compaction energy ($< 10\%$) is stored as recoverable energy. Thus, the PSK model [3], for which all compaction energy is dissipated, reasonably predicts compaction-induced dissipation for granular HMX. For small piston speeds ($u_p < 45\mathrm{m/s}$), the rate-independent dissipation term **(ii)** exceeds the rate-dependent term **(i)** which is seen to vanish in the limit $u_p \to 0$. For larger piston speeds, the rate-dependent term **(i)** constitutes an increasingly larger fraction of the total specific compaction energy.

Using the caloric equation of state $e_s = c_{vs}T + q$, with $c_{vs} = 1500\,\mathrm{J/kg/K}$ and $q = 5.84 \times 10^6\,\mathrm{J/kg}$, final bulk temperatures of less than 320 K are predicted based on bulk compaction-induced dissipation. As this temperature is far below the ignition temperature of HMX ($\sim 600\,\mathrm{K}$), the continuum model must be supplemented with a thermal energy localization model to predict ignition of granular HMX.

CONCLUSIONS

We have extended the BN-model to account for irreversible changes in the volume fraction. Our model is thermodynamically consistent and gives a more general treatment of compaction energetics than do conventional two-phase DDT models; thus, it can be applied to elastic, plastic, or brittle materials. When applied to compaction of granular HMX, the model predicts results commensurate with experiments including significant dissipation and stress relaxation. The latter is not predicted by conventional models. Future work will address the development of 1) a model

for the evolution of granular bed morphology in terms of a grain size distribution function, and 2) a model for differentially localizing energy dissipated by the compaction process in order to predict the formation of hot-spots and the evolution of their distribution.

ACKNOWLEDGMENTS

Much of this research was performed while K. A. Gonthier was a post-doctoral fellow with the group DX-2 at Los Alamos National Laboratory.

REFERENCES

1 P. Butler and H. K. Krier. Analysis of deflagration to detonation transition in high-energy solid propellants. *Combustion and Flame*, 63:31–48, 1986.

2 M. R. Baer and J. W. Nunziato. A two-phase mixture theory for the deflagration-to-detonation transition in reactive granular materials. *Int. J. Multiphase Flow*, 12:861–889, 1986.

3 J. M. Powers, D. S. Stewart, and H. K. Krier. Theory of two-phase detonation-part I: modeling. *Combustion and Flame*, 80(3):264–279, 1990.

4 J. B. Bdzil, R. Menikoff, S. F. Son, A. K. Kapila, and D. S. Stewart. Two-phase models of ddt: Review and modeling issues. *Phys. Fluids* (submitted), 1998.

5 P. J. Coyne, W. L. Elban, and M. A. Chiarito. The strain rate behavior of coarse HMX porous bed compaction. In *Proceedings of Eighth Symposium (International) on Detonation, Albuquerque, NM, July 15–19, 1985*, pages 645–657, White Oak, Silver Spring, Maryland 20903–5000, 1986. Naval Surface Weapons Center.

6 J. Kratochvil and O. W. Dillon Jr. Thermodynamics of elastic-plastic materials as a theory with internal state variables. *J. Applied Mech.*, 40(8):3207–3218, 1969.

7 J. M. Powers, D. S. Stewart, and H. Krier. Analysis of steady compaction waves in porous materials. *J. Applied Mech.*, 56:15–24, 1989.

8 M. R. Baer. Numerical studies of dynamic compaction of inert and energetic granular materials. *Journal of Applied Mechanics*, 55:36–43, 1988.

9 H. W. Sandusky and T. P. Liddiard. Dynamic compaction of porous beds. Technical Report NSWC TR 83-246, Naval Surface Weapons Center, 1985.

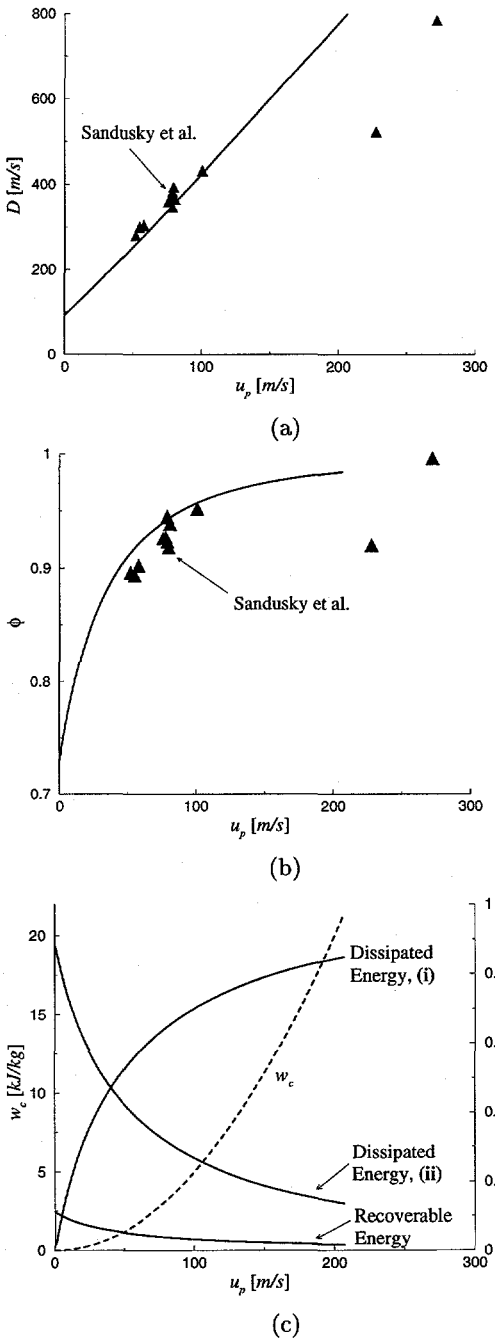

FIGURE 5. PREDICTED VARIATION IN (a) COMPACTION WAVE SPEED, (b) FINAL SOLID VOLUME FRACTION, AND (c) FINAL MASS SPECIFIC ENERGY WITH PISTON SPEED FOR DYNAMIC COMPACTION WAVES.